

The dynamic structure factor in impurity-doped spin chains

Annabelle Bohrdt^{1,2}, Kevin Jägering¹, Sebastian Eggert¹, and Imke Schneider¹

¹*Physics Department and Research Center OPTIMAS,*

University of Kaiserslautern, D-67663 Kaiserslautern, Germany and

²*Department of Physics and Institute for Advanced Study,
Technical University of Munich, 85748 Garching, Germany*

The effects of impurities in spin-1/2 Heisenberg chains are recently experiencing a renewed interest due to experimental realizations in solid state systems and ultra-cold gases. The impurities effectively cut the chains into finite segments with a discrete spectrum and characteristic correlations, which have a distinct effect on the dynamic structure factor. Using bosonization and the numerical Density Matrix Renormalization Group we provide detailed quantitative predictions for the momentum and energy resolved structure factor in doped systems. Due to the impurities, spectral weight is shifted away from the antiferromagnetic wave-vector $k = \pi$ into regions which normally have no spectral weight in the thermodynamic limit. The effect can be quantitatively described in terms of scaling functions, which are derived from a recurrence relation based on bosonization.

Spin chains have been the center of attention as prototypical quantum many body systems ever since the early days of quantum mechanics [1] and up to this day significant advances are made, e.g. in describing exact form factors [2–6], exact correlations [7], non-equilibrium states [8, 9], and dynamic correlations in the regime of a non-linear spectrum [10–18]. Recently, there has been renewed experimental interest in intentionally doped spin chain systems [19, 20] with new results on the Knight shift [21, 22], magnetic ordering [23], and the dynamic structure factor [24–27]. Doped spin chains are known to acquire characteristic boundary correlation functions [28], which lead to impurity induced changes in the Knight shift [29, 30], the susceptibility [31–33], the static structure factor [30], and the ordering temperature [34, 35]. However, surprisingly a systematic analysis of the doping effects on the energy and momentum resolved dynamic structure factor is still missing so far. Previous research has taken into account the discrete spectrum of finite chains [24, 25, 36], which leads to an exponential suppression at low energies [24, 25]. The understanding of the momentum dependence is more involved, however, since characteristic correlations near the impurities play an important role and lead to a strong redistribution of spectral weight to higher momenta outside the dispersion relation as shown in this paper.

The underlying model is the well-known xxz -spin chain

$$H = J \sum_{i=1}^{L-1} (S_i^x S_{i+1}^x + S_i^y S_{i+1}^y + \Delta S_i^z S_{i+1}^z) \quad (1)$$

which represents a one-dimensional array of L interacting spin-1/2 operators with open boundary conditions. This model can also be used to describe hard-core bosons [37], quantum dimer systems [38], or triplon excitations in ladder systems [39]. The longitudinal dynamic structure factor is a key quantity, which can be measured by angle-resolved neutron scattering experiments [40–42] and at the same time gives a deep insight into the spatial-temporal correlations. Impurities in the systems cut the

spin chains [28, 36], so we consider the structure factor for finite segments of length L

$$S(\omega, k) = \frac{1}{L} \sum_{j, j'} e^{-ik(j-j')} \int_{-\infty}^{\infty} dt e^{i\omega t} \langle S_j^z(t) S_{j'}^z(0) \rangle. \quad (2)$$

In recent years it was possible to calculate $S(\omega, k)$ to high accuracy from exact methods in the thermodynamic limit [4, 5] which is nonzero only inside the bounds of the known dispersion [43] as shown schematically in the bottom left panel of Fig. 1. Indicated in red are the dominant correlations near the antiferromagnetic wave-vector $k = \pi$ at low frequencies, which will be the topic of this paper. The low-energy behavior for infinite chains $L \rightarrow \infty$ has been known since the 1980s from bosonization [44] and is described by powerlaws as also derived in the appendix

$$S_{\infty}(\omega, q + \pi) = (2v)^{1-2K} \pi^2 A_z \Gamma^{-2}(K) (\omega^2 - v^2 q^2)^{K-1}, \quad (3)$$

where $|q| = |k - \pi| < \omega/v$, $K = \pi/2(\pi - \theta)$ is the Luttinger parameter, $v = J\pi \sin \theta/2\theta$ is the spinon velocity in terms of $\cos \theta = \Delta$ [45] and the overall amplitude A_z is known from exact methods [46]. Since $K < 1$ for $\Delta > 0$ the signal increases with ω^{2K-2} as the frequency is lowered and shows a divergence near the dispersion $\omega^2 - v^2 q^2 \rightarrow 0^+$, but vanishes for $|vq| > \omega$. A substantial amount of literature has been devoted to the analysis of the divergence at the dispersion in spin chains and quantum wires [47], which finds that it is not universal but depends on non-linear effects [10–18] as well as the cut-off procedure [48, 49]. In this work we now consider finite chains, which show no divergence at all. Remarkably, at low energies bosonization nonetheless gives quantitatively accurate results for all $q = k - \pi$ and L . It is therefore possible to perform an efficient large-scale impurity averaging to predict the experimental signal.

The low-energy spectrum of finite spin chains is well described by equally spaced energy levels $\omega_m \approx m\Delta\omega$ with $\Delta\omega = \frac{\pi v}{L}$ [28]. Higher order corrections to this

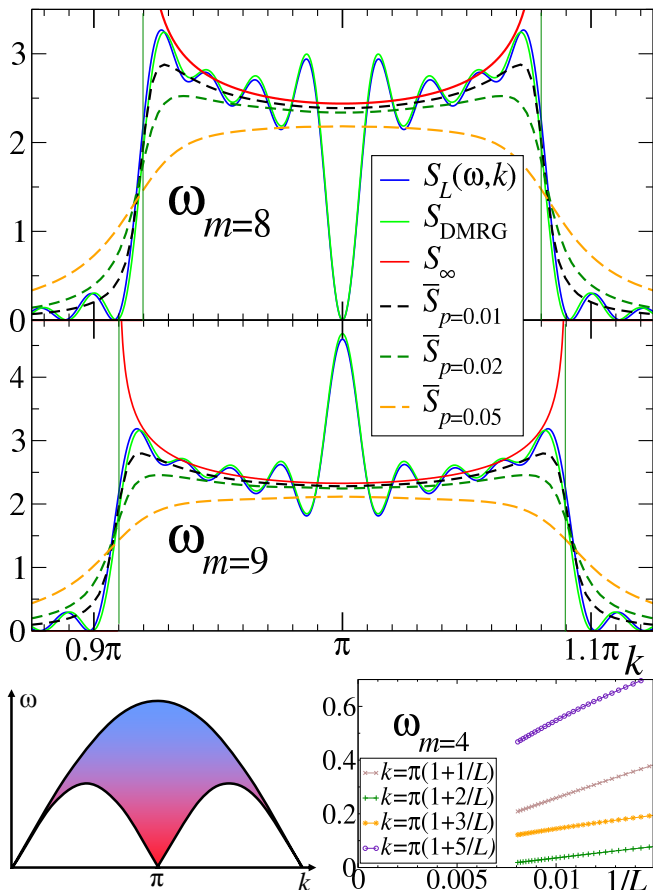


Figure 1: *Top*: The dynamical structure factor $S_L(\omega_m, k)$ at $L = 100$ as a function of k near π from bosonization compared to numerical DMRG calculations for $\omega_m = 8\pi v/L \approx 0.31J$ and $9\pi v/L \approx 0.348J$. The $L \rightarrow \infty$ behavior S_∞ from Eq. (3) and the averaged signal \bar{S}_p with doping level p at the same energies are also shown where vertical lines mark $v|k - \pi| = \omega_m$. *Bottom left*: Schematic spinon dispersion. *Bottom right*: Bosonization error over finite size deviation ΔS in Eq. (14) for $m = 4$ and different k using $K = 0.8$ as a function of $1/L$.

quantization are well understood [28, 50–52], but do not change the averaged signal. Because of the discrete spectrum it is useful to rewrite Eq. (2) in the Lehmann representation

$$S(\omega, k) = \Delta\omega \sum_{m \neq 0} S_L(\omega_m, k) \delta(\omega - \omega_m) \quad (4)$$

where we have defined individual spectral weights

$$S_L(\omega_m, k) = \frac{2\pi}{\Delta\omega} |\langle \omega_m | S_k^z | 0 \rangle|^2 \quad (5)$$

with $S_k^z = \frac{1}{\sqrt{L}} \sum_j e^{-ikj} S_j^z$. Note that the scattering wave-vectors k are not quantized.

Numerically the spectral weights $S_L(\omega_m, k)$ can be evaluated by targeting a large number of excited states in Density Matrix Renormalization Group (DMRG) simulations [53] as discussed below. Analytically it turns out that bosonization gives an accurate estimate for S_L from

a simple sum over a finite number of collective modes, which agree accurately with our DMRG simulations already for moderate lengths.

The bosonization and calculation of correlation functions of finite spin chains has been discussed before [28, 35, 51, 54, 55] as reviewed in the appendix. It is based on expressing the alternating part of the spin-operator in terms of a free bosonic field ϕ

$$S^z(x, t) \approx A(-1)^x \sin \sqrt{4\pi K} \phi(x, t), \quad (6)$$

where the amplitude $A^2 = A_z/2$ is known from exact methods [46]. Long-distance correlations can then be calculated by expectation values of the form

$$G^\pm(x, y, t) = \langle e^{i\sqrt{4\pi K} \phi(x, t)} e^{\mp i\sqrt{4\pi K} \phi(y, 0)} \rangle. \quad (7)$$

The main technical difficulty is the Fourier-transform over time in Eq. (2), which ordinarily requires a detailed analysis of the analytic structure and contour integrals with a cut-off procedure [44, 47, 56]. However, in our calculation we use finite systems, which provides an efficient way of calculating spectral weights, that can be summarized in a few lines as follows and is derived in the appendix. Due to the discrete energy spectrum, the Fourier-transform gives a sum over delta-functions

$$\int_{-\infty}^{\infty} dt G^\pm(x, y, t) e^{i\omega t} = 2\pi \sum_m S_m^\pm(x, y) \delta(\omega - \omega_m). \quad (8)$$

To evaluate the spectral weights S_m^\pm it is possible to use the mode expansion and an integration by parts of Eq. (8) to arrive at a recurrence relation [57, 58]

$$S_m^\pm(x, y) = \frac{\pm 1}{m} \sum_{\ell=1}^m S_{m-\ell}^\pm(x, y) \gamma_\ell(x, y), \quad (9)$$

which allows to express the S_m^\pm in Eq. (8) as a recursive sum of the ones with lower index $m - \ell$ using starting values of

$$S_0^+(x, y) = S_0^-(x, y) = c(x)c(y) = \left(\frac{4L^2}{\pi^2} \sin \frac{\pi x}{L} \sin \frac{\pi y}{L} \right)^{-K} \quad (10)$$

and the coefficients

$$\gamma_\ell(x, y) = 4K \sin \frac{\ell\pi x}{L} \sin \frac{\ell\pi y}{L}. \quad (11)$$

It is then straight-forward to evaluate the spatial Fourier-transform

$$S_m^\pm(k) = \frac{1}{L} \int_0^L dx \int_0^L dy e^{i(\pi-k)(x-y)} S_m^\pm(x, y), \quad (12)$$

to obtain the spectral weights S_L in Eq. (5)

$$S_L(\omega_m, k) = \frac{A_z L}{2v} (S_m^+(k) - S_m^-(k)). \quad (13)$$

In the case of odd L the integrands $S_m^\pm(x, y)$ acquire an additional factor of $\cos \pi(x \pm y)/L$ from zero modes which reflects the parity symmetries of the wavefunctions. Note that the spatial Fourier transform in Eq. (12) dominates for antiferromagnetic wavevectors $k \approx \pi$, i.e. small $q = k - \pi$. The expression for $S_m^\pm(x, y)$ from Eq. (9) contains products of different γ_ℓ with the starting value S_0^\pm , so the spatial integral in Eq. (12) can be evaluated exactly using known integrals as shown in the appendix.

In the following we use this procedure to efficiently calculate spectral weights $S_L(\omega_m, k)$ for comparison to numerics, for impurity averaging, and for extracting the asymptotic behavior for long chains. However, it has been shown before that bosonization results can strongly depend on non-linear corrections [10–18] or the cut-off procedure [48, 49], so we first critically examine if this approach gives correct results. To this end we use DMRG [53] to calculate spectral weights in finite systems. Using the multi-targeting algorithm for spectral weights [59] we can calculate the first 97 excitations, which captures all nearly-degenerate multiplets up to the energy level $m = 9$. Using $M = 600$ DMRG states gives an accuracy in the wavefunction of order 10^{-2} relative to exact results from the xx -model.

A direct comparison between bosonization S_L and numerics S_{DMRG} is shown in Fig. 1 for energy levels $m = 8$ and $m = 9$ in a finite system of $L = 100$ with $K = 0.8$. Without any fit the agreement is surprisingly accurate and even captures details like an alternating signal at $k = \pi$ with even and odd m due to parity symmetry, which leads to overall oscillations. Due to the zero-mode prefactor the same alternation is observed between even and odd lengths L . For a quantitative analysis we also compare the small error between DMRG S_{DMRG} and bosonization S_L with the finite size correction relative to the bulk behavior S_∞ in Eq. (3) by defining

$$\Delta S \equiv \frac{S_L - S_{\text{DMRG}}}{S_L - S_\infty}. \quad (14)$$

Both the numerator and the denominator go to zero as $L \rightarrow \infty$, but the error to the numerics vanishes quicker with $1/L$ as shown in the lower right panel of Fig. 1 for $m = 4$, $K = 0.8$ and selected k -values, for which the denominator tends to be small.

We are now in the position to efficiently calculate S_L for a large range of L , k , and ω to average the signal in a randomly doped system. An impurity density p of non-magnetic sites gives a distribution of chain lengths [35, 36] $P(L) = p^2(1-p)^L$ normalized so that $\sum LP(L) = 1 - p$. The averaged signal \bar{S}_p for typical experimental doping values in Fig. 1 shows that the signal at the divergence is strongly reduced relative to the undoped case $L \rightarrow \infty$ while significant spectral weight is observed just outside the dispersion $|vq| > \omega$.

It must be emphasized that the finite-size bosonization is completely divergence free. For any finite or impurity-

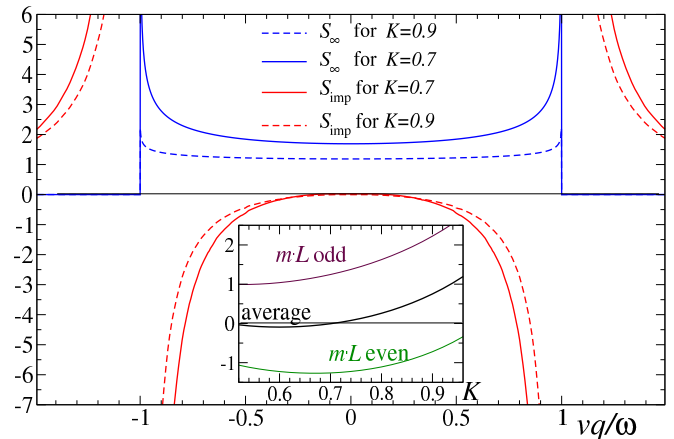


Figure 2: The rescaled signal $(\frac{\omega}{v})^{2-2K} S_\infty$ and $(\frac{\omega}{v})^{3-2K} S_{\text{imp}}$ as functions of the scaling variable vq/ω for $K = 0.7$ and $K = 0.9$. Inset: Relative impurity contribution $\omega \hat{S}_{\text{imp}}(\omega) / v \hat{S}_\infty(\omega)$ from the k -integrated signal as a function of K .

doped system we obtain a well-behaved finite signal even at $|vq| = \omega$, so it is unclear in what situation the power-law divergence in Eq. (3) becomes relevant. To answer this question we analyze the impurity correction S_{imp} relative to the thermodynamic limit, which is defined as the first order in a $1/L$ expansion [30]

$$S_L(\omega, k) = S_\infty(\omega, k) + L^{-1} S_{\text{imp}}(\omega, k) + \mathcal{O}(L^{-2}). \quad (15)$$

Based on the efficient calculation of spectral weights from Eqs. (9)-(13) we can make a comprehensive finite-size scaling to determine S_∞ and S_{imp} for different ω and k . Due to the scale-invariance of the underlying bosonization the resulting contributions in Eq. (15) show perfect data collapse, so that $\omega^{2-2K} S_\infty$ and $\omega^{3-2K} S_{\text{imp}}$ are only functions of the scaling variable vq/ω as shown in Fig. 2 for $K = 0.7$ and $K = 0.9$. While S_∞ is given by Eq. (3), we find that $S_{\text{imp}} \propto \omega^{2K-3}$ increases even faster with decreasing ω . This is reminiscent of quantum wires, which also show boundary dominated spectral functions at low energies [56]. Even more interesting is the strong divergence of the impurity part in Fig. 2, which goes as $|vq| - \omega|^{K-2}$ and implies a breakdown of the expansion in Eq. (15) as $|vq| \rightarrow \omega$. In particular, summing over higher order corrections in $1/L$ in Eq. (15) would be required as $|vq| \rightarrow \omega$ with more and more divergent powerlaws, even though the final result must be finite at the corresponding length as shown above.

Nonetheless, the expansion in Eq. (15) is useful away from the divergences in order to estimate the length-averaged signal to lowest order in p

$$\bar{S}_p(\omega, k) \approx E_1\left(\frac{p\pi v}{\omega}\right) S_\infty(\omega, k) + p E_2\left(\frac{p\pi v}{\omega}\right) S_{\text{imp}}(\omega, k), \quad (16)$$

in terms of the Einstein functions E_1 and E_2

$$E_1(x) = \frac{x^2 e^x}{(e^x - 1)^2} \quad \text{and} \quad E_2(x) = \frac{x}{e^x - 1}, \quad (17)$$

that are derived in the appendix. Both E_1 and E_2 become exponentially small for energies below the average-length gap $\omega \ll \pi v/\bar{L} \equiv p\pi v$. The suppression of bulk spectral weight with E_1 due to the finite size gaps was discussed and observed experimentally [24, 25], but we find that the additional redistribution of spectral weight becomes very important, which can be traced to the effect of boundary correlations. The rescaled average $\omega^{2-2K}\bar{S}_p$ from Eq. (16) is now a function of two scaling variables vq/ω and vp/ω . The corresponding data collapse holds approximately also for the averages over all lengths shown in Fig. 1 above, so that the signal for a given ω can easily be generalized to other energies.

The averaged signal in Fig. 1 and the impurity correction in Fig. 2 show that the signal is strongly reduced for $|vq| < \omega$, while spectral weight is created for $|vq| > \omega$. This invites the question if the k -integrated signal $\hat{S}(\omega)$ at a given energy is overall increased or decreased or even unchanged due to the boundaries. This is relevant for neutron scattering experiments, which recently observed significant changes of the spectral weight around $k \approx \pi$ depending on the doping [26, 27]. To calculate the integrated antiferromagnetic spectral weight \hat{S} as a function of L , we use the fact that an integration over k of Eq. (12) leads to delta-functions $2\pi\delta(x-y)$, so it is possible to apply the recurrence relation in Eq. (9) for $S_m^\pm(x, x)$, which is inserted into the corresponding spatial integral. Finite size scaling gives a bulk part $\hat{S}_\infty(\omega) \propto \omega^{2K-1}$ which now decreases with decreasing ω corresponding to the integral of Eq. (3). However, the impurity part $\hat{S}_{\text{imp}}(\omega) \propto \omega^{2K-2}$ increases with decreasing ω , so we define the energy independent ratio $\omega\hat{S}_{\text{imp}}(\omega)/v\hat{S}_\infty(\omega)$, which is only dependent on K (i.e. Δ) as shown in the inset of Fig. 2. Note that due to the alternation with m and L the impurity part is different if $m \cdot L$ is even or odd, but the experimentally relevant average gives a finite and relatively small value. Therefore, the corresponding expansion and averaging in Eqs. (15) and (16) work well to calculate the doping and energy dependence using the k -integrated data in Fig. 2 (inset). The impurity part becomes negative at $K \lesssim 0.7$ i.e. larger Δ , which may in part explain an additional depletion of spectral weight at low energies, but the experimentally observed changes with different impurity types [26] require more refined models beyond simple chain breaks.

Last but not least it is instructive to consider finite systems with periodic boundary conditions. The starting values in Eq. (10) are now independent of position $c = (\frac{2\pi}{L})^K$, so all integrals can be done directly. As shown in the appendix the recurrence relation leads to an analytical result for all energies, lengths, and momenta

$$S_L(\omega_m, k_l) = \frac{A_z L^2 c^2}{4v\Gamma^2(K)} \frac{\Gamma(\frac{m+l}{2} + K)}{\Gamma(\frac{m+l}{2} + 1)} \frac{\Gamma(\frac{m-l}{2} + K)}{\Gamma(\frac{m-l}{2} + 1)} \quad (18)$$

where now $\omega_m = 2\pi v m/L$ and also $k_l - \pi = 2\pi l/L$ is quantized due to periodicity with the condition that l and m are either both even or both odd integers and $|l| \leq m$. Therefore, there is no spectral weight for $v|k_l - \pi| > \omega_m$ in strong contrast to open boundary condition discussed above. It is straight-forward to expand Eq. (18) in $1/L$ using Stirlings formula to obtain S_∞ in Eq. (3) and a negative impurity part S_{imp} .

In summary we have analyzed the structure factor of doped spin chain systems. Using bosonization and numerical DMRG, we see that doping leads to a significant shift of spectral weight from lower momenta to regions $v|k - \pi| > \omega$ in neutron scattering experiments, which would not show any signal for infinite or periodic systems. The relative change from doping near the dispersion $|vq| \rightarrow \omega$ is infinitely large, so that the first order impurity contribution diverges near the dispersion $|vq| \rightarrow \omega$ with a stronger powerlaw than the bulk and a $1/L$ expansion from the thermodynamic limit always breaks down. Previous studies also found that the divergence in the thermodynamic limit is not universal, but instead strongly dependent on either the cut-off procedure [48, 49] or higher order terms and non-linear effects [10–18]. Naively, it could have been expected that bosonization works particularly well in the thermodynamic limit, but instead it turns out that the finite-size theory is much better controlled and quantitatively accurate even for $|vq| \rightarrow \omega$ as shown in Fig. 1. From a technical point of view, the mode expansion for finite systems leads to finite sums, which can be efficiently evaluated using a recurrence relation without the need for contour integral, asymptotic limits, non-linearities, or cut-off procedures.

It is fair to say that in one dimension it is always important to consider boundaries, since physical systems only contain finite chains even in the absence of doping [60]. This is especially also true for artificially created spin chains using surface structures [61, 62], ion-traps [63], or ultra-cold gases [64–66] as quantum simulators, where measurements of energy and space resolved correlations are in principle possible [67].

Finally we would also like to discuss the limitations and open questions which remain. It is known that for higher energies than considered in Fig. 1 higher order operators play a role, which lead to systematic corrections [28, 50, 51, 54]. In particular, in the limit $\Delta \rightarrow 1$ it is well known that logarithmic corrections lead to strong quantitative changes [50]. Those log-corrections have not yet been fully understood for open boundary systems [51, 54] and are beyond the scope of this paper. Nonetheless, preliminary DMRG simulations at $\Delta = 1$ show that the strong transfer of spectral weight to $v|k - \pi| > \omega$ is a robust feature.

APPENDIX

Here we review the bosonization and calculation of correlation functions for finite spin-1/2 xxz -chains

$$H = J \sum_i (S_i^x S_{i+1}^x + S_i^y S_{i+1}^y + \Delta S_i^z S_{i+1}^z) \quad (19)$$

with L sites and open or periodic boundary conditions. Using the correlation functions we want to calculate the dynamic structure factor at low frequencies and near the antiferromagnetic wave-vector $k \approx \pi$, which is given by

$$\begin{aligned} S(\omega, k) &= \frac{1}{L} \sum_{j, j'} e^{-ik(j-j')} \int_{-\infty}^{\infty} dt e^{i\omega t} \langle S_j^z(t) S_{j'}^z(0) \rangle \\ &= \Delta\omega \sum_{m \neq 0} S_L(\omega_m, k) \delta(\omega - \omega_m) \end{aligned} \quad (20)$$

where in the last line we have used the Lehmann representation using individual spectral weights

$$S_L(\omega_m, k) = \frac{2\pi}{\Delta\omega} |\langle \omega_m | S_k^z | 0 \rangle|^2 \quad (21)$$

at discrete energies $\omega_m = m\Delta\omega$.

BOSONIZATION AND CORRELATIONS FOR OPEN BOUNDARY CONDITIONS

The low-energy theory for the model in Eq. (19) is well described in the continuum limit by bosonic fields, which are rescaled by the square-root of the Luttinger parameter $K = \pi/2(\pi - \theta)$ where $\cos \theta = \Delta$ [45]. The free Hamiltonian is given by

$$H = \frac{v}{2} \int_0^L dx [\Pi(x)^2 + (\partial_x \phi(x))^2]. \quad (22)$$

where $v = J\pi \sin \theta/2\theta$ is the spinon velocity and Π is the momentum density conjugate to ϕ , $[\phi(x), \Pi(y)] = i\delta(x-y)$. Higher order corrections are well understood [28, 50–52], but are irrelevant for low energies and long chains.

We are interested in the local S^z -operators, which can be expressed in terms of the bosons

$$S^z(x, t) = \sqrt{\frac{K}{\pi}} \partial_x \phi(x, t) + A(-1)^x \sin(\sqrt{4\pi K} \phi(x, t)), \quad (23)$$

where $A^2 = A_z/2$ is related to the amplitude of the asymptotic correlation functions, that is known from exact methods [46].

Open boundaries lead to the following mode expansion of the bosonic fields [28, 35]

$$\phi(x, t) = \hat{Q} \frac{2x}{L} + \phi_{\text{osc}}(x, t) \quad (24)$$

with

$$\phi_{\text{osc}}(x, t) = \sum_{\ell=1}^{\infty} \frac{1}{\sqrt{\pi\ell}} \sin \frac{\pi\ell x}{L} \left(e^{-i\frac{\pi\ell vt}{L}} b_{\ell} + e^{i\frac{\pi\ell vt}{L}} b_{\ell}^{\dagger} \right). \quad (25)$$

The zero mode \hat{Q} is given in terms of the total magnetization

$$S^z = \int_0^L \sqrt{\frac{K}{\pi}} \partial_x \phi = 2\sqrt{\frac{K}{\pi}} \hat{Q}. \quad (26)$$

Note that those expressions agree with previous works [28, 35, 45], up to an overall phase shift ϕ_0 in the boson, which is of no consequence.

For the dynamical structure factor near $k \approx \pi$ we are interested in the alternating part of the $S^z S^z$ -correlation function

$$\langle \sin(\sqrt{4\pi K}\phi(x,t)) \sin(\sqrt{4\pi K}\phi(y,0)) \rangle = \frac{1}{2} (G^+(x,y,t) - G^-(x,y,t)) \quad (27)$$

with

$$G^\pm(x,y,t) = \langle e^{i2\pi S^z(x\mp y)/L} \rangle \langle e^{i\sqrt{4\pi K}\phi_{\text{osc}}(x,t)} e^{\mp\sqrt{4\pi K}\phi_{\text{osc}}(y,0)} \rangle. \quad (28)$$

The first factor gives different results for even chains $S^z = 0$ and for odd chains $S^z = \pm 1/2$ [35]

$$\langle e^{i2\pi S^z(x\pm y)/L} \rangle = \begin{cases} 1, & L \text{ even} \\ \cos\left(\frac{\pi(x\pm y)}{L}\right), & L \text{ odd} \end{cases} \quad (29)$$

which reflects the different parity symmetry of the wavefunctions in even and odd chains. For the second factor in Eq. (28) it is useful to apply normal ordering

$$\exp\left(i\sqrt{4\pi K}\phi_{\text{osc}}(x,t)\right) = c(x) \exp\left(i\sum_{\ell} e^{i\omega_{\ell}t} \frac{A_{\ell}^{\dagger}(x)}{\sqrt{\ell}}\right) \exp\left(i\sum_{\ell} e^{-i\omega_{\ell}t} \frac{A_{\ell}(x)}{\sqrt{\ell}}\right) \quad (30)$$

where $\omega_{\ell} = \ell\Delta\omega$ with $\Delta\omega = \frac{\pi v}{L}$ and operators [58]

$$A_{\ell}(x) = 2\sqrt{K} \sin\frac{\pi\ell x}{L} b_{\ell}. \quad (31)$$

The prefactor is given via the Baker-Campbell-Hausdorff formula by

$$c(x) = \exp\left(-\sum_{\ell} \frac{2K}{\ell} \sin^2\frac{\pi\ell x}{L}\right), \quad (32)$$

which is divergent. However, using

$$\sum_{\ell=1}^{\infty} q^{\ell}/\ell = -\log(1-q) \quad (33)$$

it is possible to capture the dependence on L and x correctly, so that only an overall factor is dependent on the regularization, which we choose to be finite by setting

$$c(x) = \left(\frac{2L}{\pi} \sin\frac{\pi x}{L}\right)^{-K}. \quad (34)$$

Therefore, upon using Baker-Campbell-Hausdorff again, the correlation functions in Eq. (28) becomes

$$G^\pm(x,y,t) = c(x)c(y) \exp\left(\sum_{\ell=1}^{\infty} \frac{\pm 1}{\ell} e^{-i\omega_{\ell}t} \gamma_{\ell}(x,y)\right) \quad (35)$$

where we introduced the commutator

$$\gamma_{\ell}(x,y) = [A_{\ell}(x), A_{\ell}^{\dagger}(y)] = 4K \sin\frac{\ell\pi x}{L} \sin\frac{\ell\pi y}{L}. \quad (36)$$

For odd chains, the additional factor in Eq. (29) must also be inserted.

At this point all information for the asymptotic behavior of the correlation function is known, which in fact can be expressed in closed form using Eq. (33) [28, 30, 35, 55]

$$G^\pm(x,y,t) = c(x)c(y) \left[\frac{\sin\frac{\pi(x+y-vt)}{2L} \sin\frac{\pi(x+y+vt)}{2L}}{\sin\frac{\pi(x-y-vt)}{2L} \sin\frac{\pi(x-y+vt)}{2L}} \right]^{\pm K} \quad (37)$$

for even L (and by including the factor in Eq. (29) for odd L). Note that we have normalized the correlation function so that

$$G^+(x,y,t) \rightarrow ((x-y)^2 - v^2t^2)^{-K} \quad (38)$$

in the thermodynamic limit away from the boundary. The overall prefactor must be determined from exact methods [46], so that the normalization in Eqs. (34) and (38) is simply a matter of convenience.

FOURIER TRANSFORM AND RECURSIVE FORMULA

To calculate the dynamical structure factor it is useful to go back to Eq. (35) in order to obtain the Fourier transformation in time. In accordance with the periodicity in t this yields an expansion in delta functions

$$\int_{-\infty}^{\infty} dt e^{i\omega t} G^{\pm}(x, y, t) = 2\pi \sum_m S_m^{\pm}(x, y) \delta(\omega - \omega_m). \quad (39)$$

where the discrete spectral weight for $\omega_m = m\Delta\omega = m\frac{\pi v}{L}$ is determined by the functions γ_l in a recursive way [58],

$$S_m^{\pm}(x, y) = \frac{\pm 1}{m} \sum_{\ell=1}^m S_{m-\ell}^{\pm}(x, y) \gamma_{\ell}(x, y). \quad (40)$$

which simply follows from partial integration. This equation defines the recursion formula, which allows to calculate any individual spectral weight as a sum of the previous ones from starting values $S_0^{\pm}(x, y) = c(x)c(y)$ (and including Eq. (29) for odd L). Note that this is much easier than an integration over Eq. (37) which would require a small imaginary cutoff for the time and a complicated contour integration.

For the spatial Fourier transform we define

$$S_m^{\pm}(k) = \frac{1}{L} \int_0^L dx \int_0^L dy e^{i(\pi-k)(x-y)} S_m^{\pm}(x, y) \quad (41)$$

where the shift of the wavevector by π follows from the alternating factor in Eq. (23). Using $S_m(k) = \frac{A_z}{4} (S_m^+(k) - S_m^-(k))$ we obtain

$$S(\omega, k) = 2\pi \sum_m S_m(k) \delta(\omega - \omega_m). \quad (42)$$

Since the integrand $S_m^{\pm}(x, y)$ in Eq. (41) only involves a sum of exponentials $\exp(i\ell_x \pi x/L)$ and $\exp(i\ell_y \pi y/L)$ according to Eqs. (36) and (40), it is possible to perform the integral for each such term analytically together with the prefactor $c(x)$ in Eq. (34) by using

$$\int_0^L dx \frac{e^{i\frac{\pi}{L}qx}}{(\sin \frac{\pi x}{L})^K} = \frac{\pi e^{i\pi q/2} 2^K L \csc(\pi K)}{\Gamma(K)\Gamma(q/2 - K/2 + 1)\Gamma(-q/2 - K/2 + 1)} \quad (43)$$

for $K < 1$ and analogously for the integration over y . In the summation of Eq. (40) we therefore keep track of the prefactors for each pair (ℓ_x, ℓ_y) for each level m and then add up the exactly known integrals as a function of k in Eq. (43) in the end.

PERIODIC BOUNDARY CONDITIONS

The recursive approach is particularly simple for periodic boundary conditions. In this case the system is translationally invariant, so that $G^+(x, y, t)$ is a function of $x - y$ and t only and $G^-(x, y, t)$ vanishes. The prefactor is constant $c(x) = c = (\frac{2\pi}{L})^K$. It is then convenient to introduce light-cone coordinates $z = vt - (x - y)$ and $\bar{z} = vt + x - y$ such that the correlation function factorizes

$$e^{-ik(x-y)} e^{i\omega t} G^+(x, y, t) = e^{iuz} e^{i\bar{u}\bar{z}} G(z)G(\bar{z}) \quad (44)$$

where k is measured relative to π and

$$G(z) = c \exp\left(\sum_{\ell} \frac{1}{\ell} e^{-i\frac{2\pi}{L}\ell z} \gamma\right) \quad (45)$$

with $\gamma = K$. The double Fourier transform in z and \bar{z} with frequencies $u = \frac{1}{2}(\frac{\omega}{v} + k)$ and $\bar{u} = \frac{1}{2}(\frac{\omega}{v} - k)$, respectively, can then be performed directly by applying the recursion formula in Eq. (40) to the contributions of right-movers and left-movers separately. Due to periodicity with L in z and \bar{z} , the values for both u and \bar{u} are quantized

$$u = \frac{2\pi}{L}n \quad \bar{u} = \frac{2\pi}{L}\bar{n} \quad (46)$$

The boundaries of the integrals transform as follows:

$$\frac{1}{L} \int_0^L dx \int_0^L dy \rightarrow \frac{1}{L} \int_0^L dy \int_{-y}^{L-y} dr = \int_0^L dr \quad (47)$$

for integrands independent of y and L -periodic in r . Furthermore we use

$$\int_0^L dr \int_{-\infty}^{\infty} dt \rightarrow \frac{1}{2v} \int_{-\infty}^{\infty} dz \int_{-z}^{2L-z} d\bar{z} = \frac{1}{2v} \int_{-\infty}^{\infty} dz \int_0^{2L} d\bar{z} \quad (48)$$

for integrands invariant under $\bar{z} \rightarrow \bar{z} + L$. Since $\gamma = K$ is independent of ℓ in Eq. (45), the recursion can be solved exactly to give a ratio of gamma functions [58], i.e.

$$\int_{-\infty}^{\infty} e^{iuz} G(z) dz = \frac{2\pi c}{\Gamma(K)} \sum_n \frac{\Gamma(n+K)}{\Gamma(n+1)} \delta\left(u - \frac{2\pi}{L}n\right) \quad (49)$$

and

$$\int_0^{2L} e^{i\bar{u}\bar{z}} G(\bar{z}) d\bar{z} = \frac{2Lc}{\Gamma(K)} \sum_{\bar{n}} \frac{\Gamma(\bar{n}+K)}{\Gamma(\bar{n}+1)} \delta_{\bar{u}, \bar{u}L/2\pi} \quad (50)$$

for the integration over \bar{z} . Now using the exact result for the asymptotic amplitude of the alternating correlation functions A_z from Ref. [46] we obtain

$$S(\omega, k) = \frac{\pi A_z L c^2}{2v\Gamma^2(K)} \sum_{n, \bar{n}} \frac{\Gamma(n+K)}{\Gamma(n+1)} \frac{\Gamma(\bar{n}+K)}{\Gamma(\bar{n}+1)} \delta\left(u - \frac{2\pi}{L}n\right) \delta_{\bar{u}, 2\pi\bar{n}/L} \quad (51)$$

$$= \frac{\pi A_z L c^2}{2\Gamma^2(K)} \sum_m \sum_{l=-m}^m \frac{\Gamma(\frac{m+l}{2}+K)}{\Gamma(\frac{m+l}{2}+1)} \frac{\Gamma(\frac{m-l}{2}+K)}{\Gamma(\frac{m-l}{2}+1)} \delta\left(\omega - \frac{2\pi vm}{L}\right) \delta_{k, 2\pi l/L} \quad (52)$$

where the sum over l goes in steps of two, so that $l = n - \bar{n}$ and $m = n + \bar{n}$ are either both even or both odd and $|l| \leq m$. Comparing with Eq. (20) we can write for quantized frequencies $\omega_m = m\Delta\omega = m\frac{2\pi v}{L}$ and momenta $k_l - \pi = l\frac{2\pi}{L}$

$$S_L(\omega_m, k_l) = \frac{A_z L^2 c^2}{4v\Gamma^2(K)} \frac{\Gamma(\frac{m+l}{2}+K)}{\Gamma(\frac{m+l}{2}+1)} \frac{\Gamma(\frac{m-l}{2}+K)}{\Gamma(\frac{m-l}{2}+1)} \quad (53)$$

Stirling's formula for large arguments Λ gives

$$\frac{\Gamma(\Lambda+K)}{\Gamma(\Lambda+1)} \approx \Lambda^{K-1} \left(1 + \frac{K(K-1)}{2\Lambda} + \mathcal{O}\left(\frac{1}{\Lambda^2}\right)\right) \quad (54)$$

so that to leading order we find the bulk behavior in the thermodynamic limit

$$S_\infty(\omega, q + \pi) = \frac{\pi^2 A_z}{2v\Gamma^2(K)} 2^{2-2K} \left(\frac{\omega^2}{v^2} - q^2\right)^{K-1} \quad \text{for } v|q| < \omega, \quad (55)$$

where we get a factor of 2 due to the fact that the quantization of k_l jumps in steps of two at a given m . The analogous analysis can be made for odd L where the prefactor in Eq. (29) basically gives the sum of two contribution with the k -quantization changed by one $l \rightarrow l \pm 1$.

INTEGRATED SPECTRAL WEIGHT

For the total spectral weight near the antiferromagnetic wave vector, we can integrate the contribution from the alternating correlation function

$$\widehat{S}(\omega) = \int dk S(\omega, k) \quad (56)$$

where the integral is taken in the vicinity of $k = \pi$. Let us also define the integrated spectral weight at discrete energies by

$$\widehat{S}(\omega) = 2\pi \sum_m \widehat{S}_m \delta(\omega - \omega_m). \quad (57)$$

with $\widehat{S}_m = \frac{A_z}{4}(\widehat{S}_m^+ - \widehat{S}_m^-)$. Integrating Eq. (41) over k generates a delta function $2\pi\delta(x - y)$ such that one spatial integration can be trivially performed and S_m simplifies to

$$\widehat{S}_m = \frac{\pi A_z}{2L} \int_0^L dx (S_m^+(x, x) - S_m^-(x, x)). \quad (58)$$

The functions $S_m^\pm(x, x)$ are generated recursively via Eq. (40). In case of periodic boundary conditions – since $\gamma_l(x, x) = 2K$ is independent of l – the recursion can again be solved exactly. From Eq. (49) we find

$$\widehat{S}_m = \frac{\pi A_z c^2}{2\Gamma(2K)} \frac{\Gamma(m + 2K)}{\Gamma(m + 1)}. \quad (59)$$

The bulk power law for the k -integrated structure factor is

$$\widehat{S}_\infty(\omega) = \frac{\pi^2 A_z}{v\Gamma(2K)} \left(\frac{\omega}{v}\right)^{2K-1}. \quad (60)$$

Note that this result can also be obtained by directly integrating Eq. (55).

AVERAGING OVER CHAIN LENGTHS

For a doping density of $p = N_{imp}/N$ missing sites, the probability of finding a linear segment of length L is [36]

$$P(L) = p^2(1 - p)^L \approx p^2 \exp(-Lp), \quad (61)$$

which is normalized so $N \sum P(L) = N_{imp}$. The probability of a single site to belong to a segment of length L is $LP(L)$ which is normalized so that $N \sum LP(L) = N - N_{imp}$, which excludes the missing sites. In the limit of large chains or small doping, the sums can be converted to integrals since the signal does not change significantly as a function of length so that $\int dL P(L) = p$ and $\int dL LP(L) = 1$.

For a segment of length L we use the Lehmann representation in Eq. (4) in order to define the average signal

$$\bar{S}(\omega, k) = \sum_L P(L) LS(\omega, k) \approx \int dL P(L) \sum_m \pi v S_L(\omega_m, k) \delta(\omega - \omega_m) \quad (62)$$

which allows us to average separately over the bulk and impurity contributions in the $1/L$ expansion from the thermodynamic limit

$$S_L(\omega_m, k) \approx S_\infty(\omega_m, k) + \frac{1}{L} S_{\text{corr}}(\omega_m, k) + \mathcal{O}\left(\frac{1}{L^2}\right). \quad (63)$$

For the bulk average we find

$$\bar{S}_\infty = \int_0^\infty dL \pi v p^2 e^{-Lp} \sum_m S_\infty(\omega_m) \delta\left(\omega - m\frac{\pi v}{L}\right) \quad (64)$$

$$= \sum_m \int_0^\infty dv p^2 \frac{m\pi^2 v^2}{v^2} e^{-pm\pi v/\nu} S_\infty(\omega) \delta(\omega - \nu) \quad (65)$$

$$= \sum_m \frac{mp^2 \pi^2 v^2}{\omega^2} e^{-pm\pi v/\omega} S_\infty(\omega) \quad (66)$$

$$= E_1(\pi v p/\omega) S_\infty(\omega). \quad (67)$$

upon using the substitution $L = \frac{\pi v m}{\nu}$ and $dL = -d\nu \frac{m\pi v}{\nu^2}$. Here

$$E_1(y) = \sum_m m y^2 e^{-my} = \frac{y^2 e^y}{(e^y - 1)^2} \quad (68)$$

is the Einstein function of the scaling variable $y = p\pi v/\omega$ which measures the "average-length" gap $v\pi/\bar{L}$ compared to ω [24, 25]. For the average impurity correction we use the same substitution $L = \frac{\pi v m}{\nu}$ and $dL = -d\nu \frac{m\pi v}{\nu^2}$

$$\bar{S}_{\text{imp}} = \int_0^\infty dL \frac{\pi v p^2 e^{-Lp}}{L} \sum_m S_{\text{imp}}(\omega_m) \delta\left(\omega - m \frac{\pi v}{L}\right) \quad (69)$$

$$= \sum_m \int_0^\infty d\nu p^2 \frac{\pi v}{\nu} e^{-p m \pi v/\nu} S_{\text{imp}}(\omega) \delta(\omega - \nu) \quad (70)$$

$$= \sum_m \frac{p^2 \pi v}{\omega} e^{-p m \pi v/\omega} S_{\text{imp}}(\omega) \quad (71)$$

$$= p E_2(\pi v p/\omega) S_{\text{imp}}(\omega). \quad (72)$$

which is proportional to p and the scaling function

$$E_2(y) = \sum_m y e^{-my} = \frac{y}{e^y - 1}. \quad (73)$$

This work was supported by the Deutsche Forschungsgemeinschaft (DFG) via the research centers SFB/TR49 and SFB/TR185 and by the Studienstiftung des deutschen Volkes.

-
- [1] H Bethe, Zur Theorie der Metalle, Z. Phys. A **71**, 205 (1931).
 - [2] J-S. Caux and J. M. Maillet, Computation of dynamical correlation functions of Heisenberg chains in a magnetic field, Phys. Rev. Lett. **95**, 077201(2005).
 - [3] J-S. Caux, R. Hagemans and J. M. Maillet, Computation of dynamical correlation functions of Heisenberg chains: the gapless anisotropic regime, J. Stat. Mech. P09003 (2005).
 - [4] J-S. Caux, H. Konno, M. Sorrell, and R. Weston, Tracking the effects of interactions on spinons in gapless Heisenberg chains, Phys. Rev. Lett. **106**, 217203 (2011).
 - [5] J-S. Caux, H. Konno, M. Sorrell, and R. Weston, Exact form-factor results for the longitudinal structure factor of the massless XXZ model in zero field, J. Stat. Mech. P01007 (2012).
 - [6] N. Kitanine, K.K. Kozlowski, J.M. Maillet, N.A. Slavnov, and V. Terras, Form factor approach to dynamical correlation functions in critical models, J. Stat. Mech. P09001 (2012).
 - [7] M. Dugave, F. Göhmann, K.K. Kozlowski, Low-temperature large-distance asymptotics of the transversal two-point functions of the XXZ chain, J. Stat. Mech. P04012 (2014).
 - [8] T. Prosen and M. Znidaric, Matrix product simulations of non-equilibrium steady states of quantum spin chains, J. Stat. Mech. P02035 (2009).

-
- [9] A. De Luca, M. Collura, and J. De Nardis, Nonequilibrium spin transport in integrable spin chains: Persistent currents and emergence of magnetic domains, Phys. Rev. B **96**, 020403(R) (2017).
 - [10] A. Imambekov and L.I. Glazman, Universal theory of nonlinear Luttinger liquids, Science **323**, 228 (2009).
 - [11] L.I. Glazman, A. Imambekov, and T.L. Schmidt, One-dimensional quantum liquids: beyond the Luttinger liquid paradigm, Rev. Mod. Phys. **84**, 1253 (2012).
 - [12] R.G. Pereira, J. Sirker, J-S. Caux, R. Hagemans, J.M. Maillet, S.R. White, and I. Affleck, Dynamical spin structure factor for the anisotropic spin-1/2 Heisenberg chain, Phys. Rev. Lett. **96**, 257202 (2006).
 - [13] R.G. Pereira, J. Sirker, J-S. Caux, R. Hagemans, J.M. Maillet, S.R. White and I. Affleck, Dynamical structure factor at small q for the XXZ spin-1/2 chain, J. Stat. Mech. P08022 (2007).
 - [14] R.G. Pereira, S.R. White, and I. Affleck, Exact edge singularities and dynamical correlations in spin-1/2 chains, Phys. Rev. Lett. **100**, 027206 (2008).
 - [15] V. Cheianov and M. Pustilnik, Threshold singularities in the dynamic response of gapless integrable models, Phys. Rev. Lett. **100**, 126403 (2008).
 - [16] C. Karrasch, R.G. Pereira, and J. Sirker, Low temperature dynamics of nonlinear Luttinger liquids, New J. Phys. **17**, 103003 (2015).
 - [17] I.S. Eliens, F.B. Ramos, J.C. Xavier, and R.G. Pereira, Boundary versus bulk behavior of time-dependent correlation functions in one-dimensional quantum systems, Phys. Rev. B **93**, 195129 (2016).
 - [18] H. Karimi and I. Affleck, Transverse spectral functions and Dzyaloshinskii-Moriya interactions in XXZ spin chains, Phys. Rev B **84**, 174420 (2011).
 - [19] K. Karmakar and S. Singh, Finite-size effects in the quasi-one-dimensional quantum magnets Sr₂CuO₃, Sr₂Cu_{0.99}M_{0.01}O₃ (M=Ni,Zn), and SrCuO₂,

- Phys. Rev. B **91**, 224401 (2015).
- [20] F. Hammerath, E. M. Brünig, S. Sanna, Y. Utz, N. S. Beesetty, R. Saint-Martin, A. Revcolevschi, C. Hess, B. Büchner, and H.-J. Grafe, Spin gap in the single spin-1/2 chain cuprate $\text{Sr}_{1.9}\text{Ca}_{0.1}\text{CuO}_3$, Phys. Rev. B **89**, 184410 (2014).
- [21] Y. Utz, *et al.*, Effect of different in-chain impurities on the magnetic properties of the spin chain compound SrCuO_2 probed by NMR, Phys. Rev. B **96**, 115135 (2017).
- [22] Y. Utz, *et al.*, Suppression of the impurity-induced local magnetism by the opening of a spin pseudogap in Ni-doped Sr_2CuO_3 , Phys. Rev. B **92**, 060405 (2015).
- [23] G. Simutis, *et al.*, Magnetic ordering in the ultrapure site-diluted spin chain materials $\text{SrCu}_{1-x}\text{Ni}_x\text{O}_2$, Phys. Rev. B **93**, 214430 (2016).
- [24] G. Simutis, *et al.*, Spin Pseudogap in Ni-Doped SrCuO_2 , Phys. Rev. Lett. **111**, 067204 (2013).
- [25] G. Simutis, *et al.*, Spin pseudogap in the $S=1/2$ chain material Sr_2CuO_3 with impurities, Phys. Rev. B **95**, 054409 (2017).
- [26] K. Karmakar, M. Skoulatos, G. Prando, B. Roessli, U. Stuhr, F. Hammerath, C. Rüegg, and S. Singh, Effects of quantum spin-1/2 impurities on the magnetic properties of zigzag spin chains, Phys. Rev. Lett. **118**, 107201 (2017).
- [27] K. Karmakar, R. Bag, M. Skoulatos, C. Rüegg, and S. Singh, Impurities in the weakly coupled quantum spin chains Sr_2CuO_3 and SrCuO_2 , Phys. Rev. B **95**, 235154 (2017).
- [28] S. Eggert and I. Affleck, Magnetic impurities in half-integer Heisenberg antiferromagnetic chains, Phys. Rev. B **46**, 10866 (1992).
- [29] J. Sirker and N. Laflorencie, NMR Response in quasi one-dimensional Spin-1/2 antiferromagnets, Europhys. Lett. **86**, 57004 (2009).
- [30] S. Eggert and I. Affleck, Impurities in $S=1/2$ Heisenberg antiferromagnetic chains: Consequences for neutron scattering and Knight shift, Phys. Rev. Lett. **75**, 934 (1995).
- [31] S. Fujimoto and S. Eggert, Boundary susceptibility in the spin-1/2 chain: Curie like behavior without magnetic impurities, Phys. Rev. Lett. **92**, 037206 (2004).
- [32] J. Sirker, N. Laflorencie, S. Fujimoto, S. Eggert, I. Affleck, Chain breaks and the susceptibility of $\text{Sr}_2\text{Cu}_{1-x}\text{Pd}_x\text{O}_{3+d}$ and other doped quasi one-dimensional antiferromagnets, Phys. Rev. Lett. **98**, 137205 (2007).
- [33] J. Sirker, S. Fujimoto, N. Laflorencie, S. Eggert, I. Affleck, Thermodynamics of impurities in the anisotropic Heisenberg spin-1/2 chain, J. Stat. Mech. P02015 (2008).
- [34] K.M. Kojima, *et al.*, Reduction of ordered moment and Néel temperature of quasi-one-dimensional antiferromagnets Sr_2CuO_3 and Ca_2CuO_3 , Phys. Rev. Lett. **78**, 1787 (1997).
- [35] S. Eggert, I. Affleck, and M. D. P. Horton, Néel order in doped quasi one-dimensional antiferromagnets, Phys. Rev. Lett. **89**, 047202 (2002).
- [36] S. Wessel and S. Haas, Excitation spectra and thermodynamic response of segmented Heisenberg spin chains, Phys. Rev. B **61**, 15262 (2000).
- [37] B. Paredes, A. Widera, V. Murg, O. Mandel, S. Fölling, I. Cirac, G.V. Shlyapnikov, T.W. Hänsch, I. Bloch, Tonks-Girardeau gas of ultracold atoms in an optical lattice, Nature **429**, 277 (2004).
- [38] B. Schmidt, M. Bortz, S. Eggert, M. Fleischhauer, and D. Petrosyan, Attractively bound pairs of atoms in the Bose-Hubbard model and antiferromagnetism, Phys. Rev. A **79**, 063634 (2009).
- [39] K.P. Schmidt and G.S. Uhrig, Excitations in one-dimensional $s = 1/2$ quantum antiferromagnets. Phys. Rev. Lett. **90**, 227204 (2003); Spectral properties of magnetic excitations in cuprate two-leg ladder systems, Mod. Phys. Lett. B **19**, 24 (2005).
- [40] B. Lake, D.A. Tennant, C.D. Frost, and S.E. Nagler, Quantum criticality and universal scaling of a quantum antiferromagnet, Nat. Mater. **4**, 329 (2005).
- [41] B. Lake, D. A. Tennant, and S. E. Nagler, Longitudinal magnetic dynamics and dimensional crossover in the quasi-one-dimensional spin-1/2 Heisenberg antiferromagnet KCuF_3 , Phys. Rev. B **71**, 134412 (2005).
- [42] B. Lake, D. A. Tennant, J.-S. Caux, T. Barthel, U. Schollöck, S. E. Nagler, and C. D. Frost, Multispinon continua at zero and finite temperature in a near-ideal Heisenberg chain, Phys. Rev. Lett. **111**, 137205 (2013).
- [43] J.d. Cloizeaux and J.J. Pearson, Spin-wave spectrum of the antiferromagnetic linear chain, Phys. Rev. **128**, 2131 (1962).
- [44] H.J. Schulz, Phase diagrams and correlation exponents for quantum spin chains of arbitrary spin quantum number, Phys. Rev. B **34**, 6372 (1986).
- [45] For a review on bosonization see: T. Giamarchi, *Quantum Physics in One Dimension*, Oxford Univ. Press (Oxford 2003).
- [46] S. Lukyanov and V. Terras, Long-distance asymptotics of spin-spin correlation functions for the XXZ spin chain, Nucl. Phys. B **654**, 323 (2003).
- [47] V. Meden and K. Schönhammer, Spectral functions for the Tomonaga-Luttinger model, Phys. Rev. B **46**, 15753 (1992).
- [48] V. Meden, Nonuniversality of the one-particle Green's function of a Luttinger liquid, Phys. Rev. B **60**, 4571 (1999).
- [49] L. Markhof and V. Meden, Spectral function of the Tomonaga-Luttinger model revisited: Power laws and universality, Phys. Rev. B **93**, 085108 (2016).
- [50] I. Affleck, D. Gepner, H.J. Schulz and T. Ziman, Critical behaviour of spin-s Heisenberg antiferromagnetic chains: analytic and numerical results, J. Phys. A: Math. Gen., **22**, 4725 (1990).
- [51] J. Sirker and M. Bortz, The open XXZ-chain: Bosonisation, Bethe ansatz and logarithmic corrections, J. Stat. Mech. P01007 (2006).
- [52] M. Bortz, M. Karbach, I. Schneider, and S. Eggert, Lattice vs. continuum theory of the periodic Heisenberg chain, Phys. Rev. B **79**, 245414 (2009).
- [53] S.R. White, Density matrix formulation for quantum renormalization groups, Phys. Rev. Lett. **69**, 2863 (1992); Density-matrix algorithms for quantum renormalization groups, Phys. Rev. B **48**, 10345 (1993).
- [54] I. Affleck and S. Qin, Logarithmic corrections in quantum impurity problems, J. Phys. A **32**, 7815 (1999).
- [55] A.E. Mattsson, S. Eggert, and H. Johannesson, Properties of a Luttinger liquid with boundaries at finite temperature and size, Phys. Rev. B **56**, 15615 (1997).
- [56] S. Eggert, H. Johannesson, and A. Mattsson, Boundary effects on spectral properties of interacting electrons in one dimension, Phys. Rev. Lett. **76**, 1505 (1996).
- [57] K. Schönhammer and V. Meden, Nonuniversal spectral properties of the Luttinger liquid, Phys. Rev. B **47**, 16205 (1993).

- [58] I. Schneider and S. Eggert, Recursive method for the density of states in one dimension, *Phys. Rev. Lett.* **104**, 036402 (2010).
- [59] I. Schneider, A. Struck, M. Bortz and S. Eggert, Local density of states for individual energy levels in finite quantum wires, *Phys. Rev. Lett.* **101**, 206401 (2008)
- [60] M. Takigawa, N. Motoyama, H. Eisaki, and S. Uchida, Field-induced staggered magnetization near impurities in the $S=1/2$ one-dimensional Heisenberg antiferromagnet Sr_2CuO_3 , *Phys. Rev. B* **55**, 14129 (1997).
- [61] X. Chen, *et al.*, Probing superexchange interaction in molecular magnets by spin-flip spectroscopy and microscopy, *Phys. Rev. Lett.* **101**, 197208 (2008).
- [62] C.F. Hirjibehedin, C.P. Lutz, A.J. Heinrich, Spin coupling in engineered atomic structures, *Science* **312**, 1021 (2006).
- [63] D. Porras and J. I. Cirac, Effective quantum spin systems with trapped ions, *Phys. Rev. Lett.* **92**, 207901 (2004).
- [64] T.A. Hilker, G. Salomon, F. Grusdt, A. Omran, M. Boll, E. Demler, I. Bloch, and C. Gross, Revealing hidden antiferromagnetic correlations in doped Hubbard chains via string correlators, *Science* **357**, 484 (2017).
- [65] A. Vogler, R. Labouvie, G. Barontini, S. Eggert, V. Guarnera, and H. Ott, Dimensional phase transition from an array of 1D Luttinger liquids to a 3D Bose-Einstein condensate *Phys. Rev. Lett.* **113**, 215301 (2014).
- [66] A. Mazurenko, C.S. Chiu, G. Ji, M.F. Parsons, M. Kanasz-Nagy, R. Schmidt, F. Grusdt, E. Demler, D. Greif, and M. Greiner, A cold-atom Fermi-Hubbard antiferromagnet *Nature* **545**, 462 (2017).
- [67] A. Bohrdt and D. Greif and E. Demler and M. Knap and F. Grusdt, Angle-resolved photoemission spectroscopy with quantum gas microscopes, preprint arXiv:1710.08925 (2017).